

High-resolution 2D plasmonic fan-out realized by subwavelength slit arrays

Qian Wang¹, Jing Bu² and X.-C. Yuan^{2,*}

¹ School of Electrical & Electronic Engineering, Nanyang Technological University, Nanyang Avenue, 639798, Singapore

² Institute of Modern Optics, Key Laboratory of Optoelectronic Information Science & Technology, Ministry of Education of China, Nankai University, Tianjin, 300071, China

*xcyuan@nankai.edu.cn

Abstract: The authors demonstrate a two dimensional (2D) plasmonic fan-out spot array by using subwavelength sized slit arrays. Near field scanning optical microscope (NSOM) is employed to examine intensity distributions of the generated fan-out plasmonic spots, showing good agreement with finite-difference time-domain (FDTD) simulation results. The plasmonic fan-out spots with full width half-maximum (FWHM) of $0.34\lambda_0$ are optimized by various design parameters associated with the subwavelength slit as well as polarization states.

© 2010 Optical Society of America

OCIS codes: (240.6680) Surface plasmons; (050.6624) Subwavelength structures

References and links

1. E. Ozbay, "Plasmonics: merging photonics and electronics at nanoscale dimensions," *Science* **311**(5758), 189–193 (2006).
2. W. L. Barnes, A. Dereux, and T. W. Ebbesen, "Surface plasmon subwavelength optics," *Nature* **424**(6950), 824–830 (2003).
3. J. R. Krenn, H. Ditlbacher, G. Schider, A. Hohenau, A. Leitner, and F. R. Aussenegg, "Surface plasmon micro- and nano-optics," *J. Microscopy-Oxford* **209**, 167 (2003).
4. S. Kawata, Y. Inouye, and P. Verma, "plasmonics for near-field nano-imaging and superlensing," *Nat. Photonics* **3**(7), 388–394 (2009).
5. L. Pang, G. M. Hwang, B. Slutsky, and Y. Fainman, "Spectral sensitivity of two-dimensional nanohole array surface plasmon polariton resonance sensor," *Appl. Phys. Lett.* **91**(12), 123112 (2007).
6. J. A. Dionne, K. Diest, L. A. Sweatlock, and H. A. Atwater, "PlasMOSStor: a metal-oxide-Si field effect plasmonic modulator," *Nano Lett.* **9**(2), 897–902 (2009).
7. D. Gao, W. Chen, A. Mulchandani, and J. S. Schultz, "Detection of tumor markers based on extinction spectra of visible light passing through gold nanoholes," *Appl. Phys. Lett.* **90**(7), 073901 (2007).
8. H. Raether, *Surface Plasmons on Smooth and Rough Surfaces and on Gratings*, (Springer, Berlin, 1988).
9. L. Feng, K. A. Tetz, B. Slutsky, V. Lomakin, and Y. Fainman, "Fourier plasmonics: Diffractive focusing of in-plane surface plasmon polariton waves," *Appl. Phys. Lett.* **91**(8), 081101 (2007).
10. A. Drezet, A. Hohenau, A. L. Stepanov, H. Ditlbacher, B. Steinberger, F. R. Aussenegg, A. Leitner, and J. R. Krenn, "Surface plasmon polariton Mach-Zehnder interferometer and oscillation fringes," *Plasmonics* **1**(2-4), 141–145 (2006).
11. B. Lamprecht, J. R. Krenn, G. Schider, H. Ditlbacher, M. Salerno, N. Felidj, A. Leitner, F. R. Aussenegg, and J. C. Weeber, "Surface plasmon propagation in microscale metal stripes," *Appl. Phys. Lett.* **79**(1), 51–53 (2001).
12. P. Ehbets, H. P. Herzig, D. Prongué, and M. T. Gale, "High-efficiency continuous surface-relief gratings for two-dimensional array generation," *Opt. Lett.* **17**(13), 908–910 (1992).
13. D. C. Su, J. T. Chang, and Y. T. Huang, "1-to-(N N) optical fan-out module for optical interconnects," *J. Opt.* **28**(2), 70–73 (1997).
14. J. W. Goodman, "Fan-in and Fan-out with Optical Interconnections," *J. Mod. Opt.* **32**(12), 1489–1496 (1985).
15. H. Gao, J. Henzie, and T. W. Odom, "Direct evidence for surface plasmon-mediated enhanced light transmission through metallic nanohole arrays," *Nano Lett.* **6**(9), 2104–2108 (2006).
16. P. Lalanne, J. P. Hugonin, and J. C. Rodier, "Theory of surface plasmon generation at nanoslit apertures," *Phys. Rev. Lett.* **95**(26), 263902 (2005).
17. N. C. Lindquist, A. Lesuffleur, and S. H. Oh, "Lateral confinement of surface plasmons and polarization-dependent optical transmission using nanohole arrays with a surrounding rectangular Bragg resonator," *Appl. Phys. Lett.* **91**(25), 253105 (2007).

1. Introduction

Typical structural sizes of photonic devices in dielectric material are much greater than electronic ones. Plasmonics enabled possibilities of the photonic devices to be functional

at subwavelength dimensions. Surface plasmon polaritons (SPP) waves are essentially one kind of electromagnetic surface waves and are confined on the metal/dielectric interface. Their unique properties provide a novel way to combine the advantages of photonics and electronics in developing the plasmonic components and systems which have similar sizes as the current integrated circuits [1]. There have been great interests in the study of subwavelength structures for maneuvering SPP waves [2,3]. Ultimately it may be possible to employ plasmonic components to form building blocks of chip-based optical device technologies, for various applications in imaging [4], spectroscopy [5], interconnection in computing, communication [6] and chemical/biological detection [7]. Previous studies show that SPP's behavior on metal surface is similar to light waves in two dimensional spaces [8]. This means that plasmonic elements and/or components can possibly be realized by employing the same ingenious principle, such as focusing [9], beam splitting [10] and wave-guiding [11].

A traditional fan-out element splits a single beam into quasi plane waves by using phase gratings and lenses to generate an array of light spots. Such space-invariant fan-out elements are widely used in parallel processing systems [12–14]. In this Paper, we report on implementation of two-dimensional (2D) plasmonic fan-out by employing optimized subwavelength slit arrays on the metal film. The optimized fan-out spot has the subwavelength sized FWHM, and is confined on the metal surface. These unique properties make it possible to be utilized in high integration plasmonic circuit.

2. Principle of the plasmonic fan-out element

SPP waves are essentially electromagnetic surface waves confined on the dielectric/metal interface. The wavevector of the SPP is matched by the metallic surface based on its dispersion relation, and will therefore depend on the frequency of incident light and the dielectric functions of the metal and the analyte [7]. For a given metallic material, the wavevector of SPP, k_{sp} can be expressed as

$$k_{sp} = k_0 \sqrt{\frac{\epsilon_m \epsilon_d}{\epsilon_m + \epsilon_d}} \quad (1)$$

where k_0 is the wavevector of the incident light; ϵ_m and ϵ_d are the permittivities of metal and dielectric material, respectively. In our designated experiment conditions, the resonant condition can simply be modulated by the pitch of surface structure with different metal/analyte configurations to meet the resonant requirements. Subwavelength sized slit is optimized to get highest SPP generation efficiency. Diffraction through the subwavelength slit on metal film can directly provide coupling of the momentum between far-field illumination and SPPs, under the condition that

$$k_{sp} = k_{//} \pm mG \quad (2)$$

where $k_{//}$ is the illuminated wavevector component along metal surface, m is an integer and the structure momentum $G = 2\pi/\Lambda$, is varied by the surface structure pitch Λ [8].

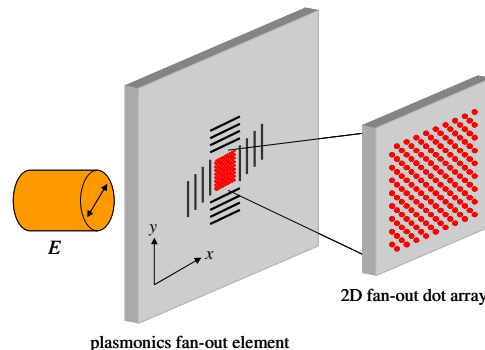


Fig. 1. (Color online) Plasmonic fan-out spot array read out

As illustrated in Fig. 1, the plane waves of electromagnetic waves emanate from the objective lens and normally incident on the metal film. Optimized subwavelength slit arrays are embedded on the metal film to generate the SPP waves with wavevector of $\pm k_{sp}$ in both vertical and horizontal directions. These SPP waves traveling in four opposite and perpendicular directions propagate towards the center of the sample and interfere to form the fan-out dot array. Working principle of the plasmonic fan-out element can be classified into two parts: (1) subwavelength slit arrays is used to generate SPP waves propagating along the metal surface, and (2) four perpendicular counter-propagating SPP waves interfered each other to form the localized plasmonic dots array. The advantage of this technology is the structure can simply be written on one chip in nanometer scale, thus integrate such an element in a chipset system can further reduce the size of plasmonic circuits.

3. Simulation and experimental results

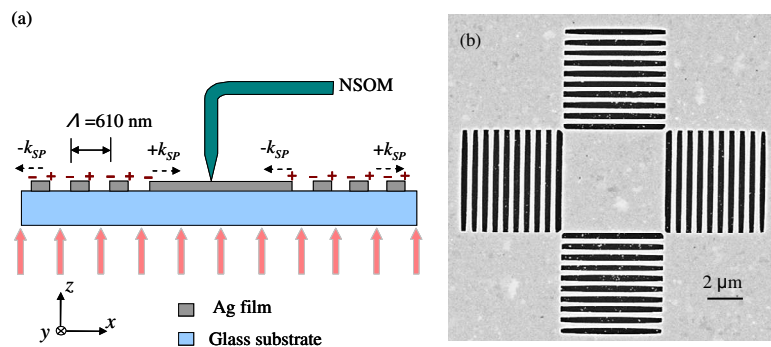


Fig. 2. (Color online) (a) Schematic of subwavelength slit arrays structure. (b) SEM image of structure.

As depicted in Fig. 2(a), our proposed structure consists of silver (Ag) as a metal thin film, subwavelength slit arrays as SPP generators and quartz glass as the substrate. Thickness of the Ag film is 100 nm, which is thick enough to block the direct transmitted light, ensuring that all fields at the Ag/dielectric interface beyond the slit area are originated from SPP waves [15]. The pitch of the slit arrays structure is 610 nm in order to match the SPP momentum for normally incident illumination with wavelength 633 nm as described in Eq. (2). The optimized width of each slit is 265 nm in order to get highest SPP generation efficiency. The proposed subwavelength slits are estimated to convert the incident light to SPP waves with 40% efficiency [16]. The structure are fabricated by electron beam lithography (EBL) (Raith e_LiNE) followed by thermal evaporation and lift-off processes. A Scanning Electron Microscopy (SEM) image of the structure is shown in Fig. 2(b). Separation between two parallel slit arrays is set as 6 μm , which is much smaller than the propagation length of SPP for Ag with dielectric constant of $-15.87 + i1.07$ in order to sustain the uniformity of the fan-out pattern.

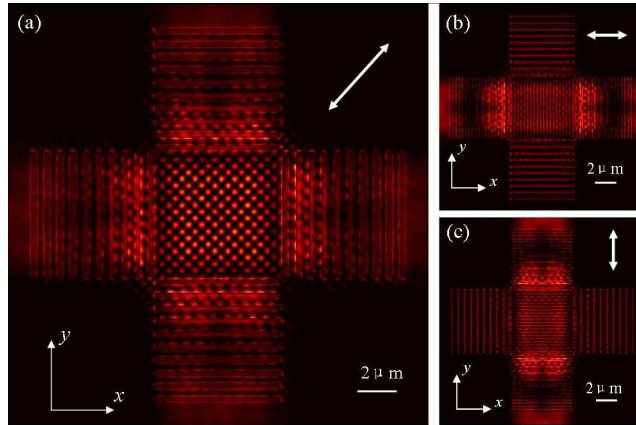


Fig. 3. (Color online) FDTD simulation results of plasmonic dot array on the planes located $z = 20$ nm above metal film along the propagating direction. The white arrow indicates the incident polarization direction along (a) diagonal direction (b) x direction, and (c) y direction.

Digital simulate calculation is carried out using a method based on the finite-difference time-domain (FDTD) (Remcom XFDFD). Simulation results of the electromagnetic intensity distribution on the plane located at 20 nm above the silver surface are shown in Fig. 3. When the linearly light incident on the sample with the polarization direction along diagonal direction (indicated by white arrow), the SPP pattern in the form of a 9×18 dot array is generated in the central area of the designed slit array structure, as shown in Fig. 3(a). Since the SPP waves can only be excited by p-polarized incident light, the diagonal polarization incident light can act as the combination of two distinguished light with x and y polarization direction, respectively. The counting propagation SPP waves are excited by x polarized light and interfere to form 1D standing SPP pattern along horizontal direction, as shown in Fig. 2(b). Similarly, y polarized light can be used to generate 1D standing SPP pattern along vertical direction at the same time, as shown in Fig. 3(c). As a result, due to the overlapping of amplitude and phase of these two direction 1D standing SPP pattern, fan-out spot array is assembled along diagonal direction in the center area. For illustration purpose, m line in x direction times n row in y direction is used to express the dot array distribution.

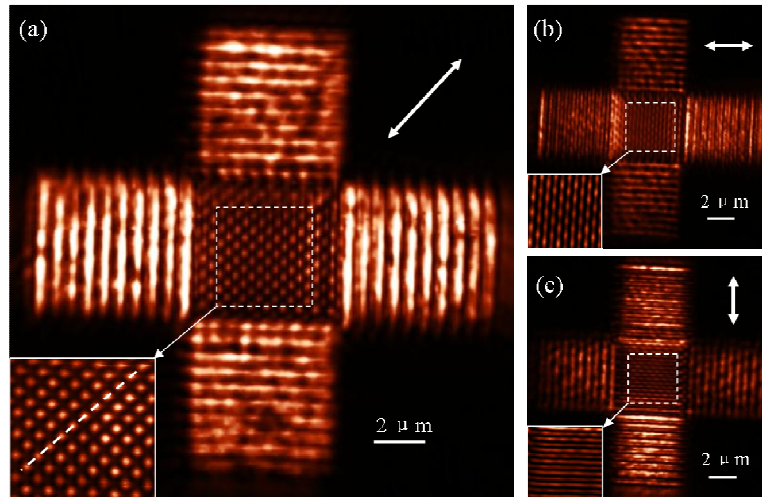


Fig. 4. (Color online) 2D Near field images of electrical field distributions for polarization direction along (a) diagonal direction (b) x direction, and (c) y direction. Insets are the SPP field intensity distribution of the structure's centre area. The white arrow indicates the incident polarization direction.

In our experiment, a linearly polarized He-Ne laser at a wavelength of 633 nm is guided into an inverted microscope and normally incident on the backside of the substrate by an objective lens with $N.A.$ equal to 0.13, where $N.A.$ is the numerical aperture of objective lens. The polarization direction of the incident light is adjusted by a half-wave plate to modulate the localized field of SPP pattern. Near field characteristics of the SPP pattern is investigated by a near-field scanning optical microscope (NSOM) (NT-MDT NTEGRA Solaris) with an aluminum coated fiber tip (nominal aperture size of 100 nm). The NSOM system is based on a tuning fork feedback mechanism to regulate the probe-sample distance in several nanometer scales. Figure 4(a) shows the experimental result of 9×18 plasmonic fan-out array. When linearly polarized light (aligned in diagonal direction) incident on the sample, the four perpendicular counter-propagating SPP waves in both $\pm x$ and $\pm y$ directions interfere with each other. A 2D standing SPP pattern which assembled in the fan-out dot array is generated in the center area of structure. 1D interference pattern in either the $\pm x$ or $\pm y$ directions due to linearly polarization light in x or y direction is used, shown in Fig. 4(b) and 4(c), respectively. The interference and the symmetry of the pattern are well agreed with the simulation result by using the FDTD calculation as shown in Fig. 3. Owing to the excitation of the SPP field at the subwavelength slits, we can observe that transmission of the corresponding slit arrays and the SPP fields at adjacent edges are significantly enhanced. The orientation along the direction of polarization explains that the SPP waves can be only excited when the polarization direction of the incident light is perpendicular to the dielectric/metal slit,

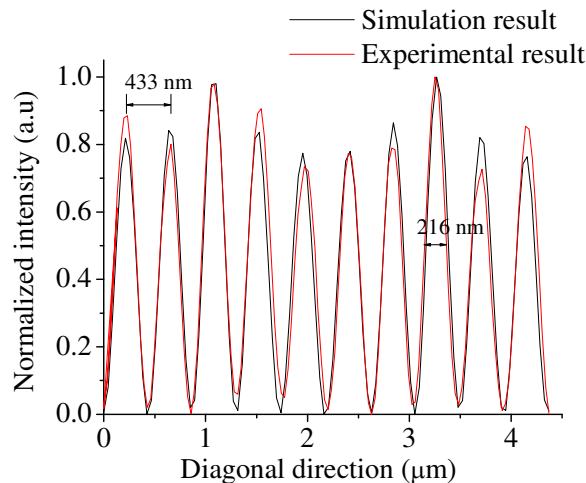


Fig. 5. Measured intensity profile of experimental and simulation line profile of the plasmonic spot array in diagonal direction.

which is p-polarized. Figure 5 shows both simulation and experimental results of cross section of the fan-out dot array extracted from the centre area of structure. The experimental result of the array period in diagonal polarization approximately equals to 438 ± 5 nm, with FWHM of 215 ± 5 nm. This interpretation is confirmed by FDTD simulation result. Another noteworthy point to mention is that the $m \times n$ dot array can be controlled by the size of center area. In our designed pattern, $6 \mu\text{m} \times 6 \mu\text{m}$ area will form 9×18 dot array. In order to generate the high density $m \times n$ plasmonic spot array, we can modulate the dimension of the centre area with the relationship of $m = \text{int}(l/\lambda_{SP})$ and $n = \text{int}(2w/\lambda_{SP})$, where $l \times w$ is the centre area size. In practice, the fan-out efficiency is decided by the intensity of located SPP pattern. One way to enhance the SPP generation efficiency is the optimization of the structure parameters, such as subwavelength slit numbers, metal thickness and slit width. Another way is to reduce SPP propagation loss by using a plasmonic cavity [17] and symmetric dielectric condition in the future work.

4. Conclusion

In summary, we have shown that a 9×18 plasmonic fan-out array can be generated with FWHM of $0.34\lambda_0$ in a very small thin metal film area using subwavelength slit arrays. Near-field scanning electromagnetic distribution is measured experimentally by an NSOM. The localized high-resolution SPP spot array is confined in an intrinsically thin region of the interface which makes it possible to apply in quasi two dimensional subwavelength size plasmonic chips. The detector array integrated on the metal surface is possible to be designed to directly collect near field fan-out pattern signal to establish a plasmonic circuit system. Furthermore, with such an SPP excitation nature, manipulation of SPP is possible by introducing more complex sub-wavelength structures, which leads towards investigation and design of more complex plasmonic devices.

Acknowledgments

This work was partially supported by the National Natural Science Foundation of China under Grant No. (10974101 and 60778045), Ministry of Science and Technology of China under Grant no.2009DFA52300 for China-Singapore collaborations and National Research Foundation of Singapore under Grant No. NRF-G-CRP 2007-01.